AUXILIARY MEDIA REVISITED – NEW INSIGHTS AND APPLICATIONS

B. Schwarz, C. Vanelle, and D. Gajewski

email: *benjamin.schwarz@uni-hamburg.de*
keywords: *time imaging, stacking, normal moveout*

ABSTRACT

In many present-day applications in seismic processing, the assumption of a homogeneous model leads to simple yet powerful approximations, which also work well when heterogeneity is not negligible. While the classical CMP stack assumes an effective constant velocity medium, de Bazelaire, based on optical projections, introduced an alternative way to account for heterogeneity by shifting the reference time rather than the velocity. In this work, we provide new insights into the auxiliary media concept by introducing forward and inverse transformations between the effective and the optical domain, and thus generalize the view on currently used stacking approximations. Supported by synthetic tests, we reveal that all higher order operators can be described in and transformed between both domains, which, through combined use suggest interesting new applications, for, e. g., wavefield characterization, separation, or passive seismic source time inversion.

INTRODUCTION

In contrast to depth imaging, approximations in time allow for efficient and robust workflows, which in areas of moderate lateral complexity can lead to a reasonable degree of accuracy. The main benefit of imaging in time is the principal independence of a user-provided velocity model, which forms the crucial ingredient for processing in depth (e. g., Landa, 2007). Being based on the assumption of local coherence of the recorded wavefield, stacking techniques can be employed in a purely data-driven fashion. While in complex settings the requirement of local coherence is not always fulfilled, data acquired in regions with moderate lateral velocity changes can be described reasonably well with analytic traveltime operators. Exploiting the main benefit of the locally coherent summation of traces, stacking can lead to a significant increase of the signal-to-noise ratio (Mayne, 1962; Jäger et al., 2001). In addition, the involved optimization process results in wavefield attribute estimates, which can be utilized for subsequent processing steps including inversion.

As a generalization of the classical CMP stack by Mayne (1962), the common-reflection-surface (CRS) stack (Jäger et al., 2001; Mann, 2002) makes optimal use of the redundancy of information in the acquired data. Although a parabolic traveltime formula, which can be seen as a truncated Taylor series expansion of the traveltime, seems to be the most intuitive choice, applications to synthetic and field data have suggested that a hyperbolic operator usually results in a better fit (e. g., Schleicher et al., 1993; Jäger, 2011). Because more complex settings are nowadays encountered in hydrocarbon exploration, diffractions and other highly curved subsurface features become increasingly important. In addition, due to the respective high angle coverage, diffractions are thought to contain super-resolved information about the subsurface (Khaidukov et al., 2004) and are strong indicators of fault structures.

Fomel and Grechka (2001) concluded that even for a homogeneous background, the description of diffracted traveltimes is a higher-order problem and, in non-local vicinities, cannot be accurately described by hyperbolic or parabolic operators. Due to this nonhyperbolicity of diffractions and traveltimes from highly curved reflectors, efforts have been made to derive higher-order traveltime approximations (e.g.,

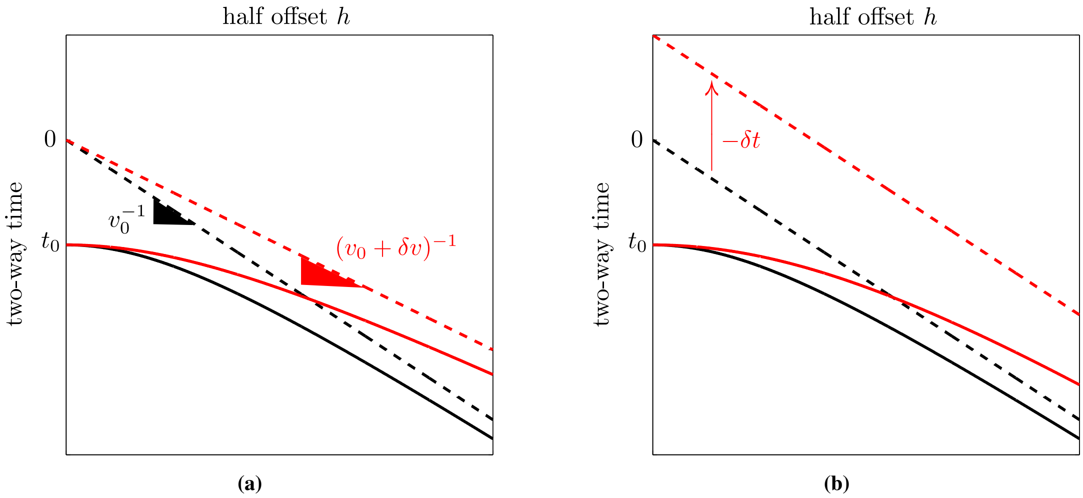

Figure 1: Two different ways to change the CMP moveout to account for heterogeneity: (a) Classical approach, where the velocity is perturbed. (b) Application of a shift δt to the reference time t_0. Actual traveltime curves are in bold lines, their respective asymptotes are dotted. In both cases red color indicates the perturbed moveout.

Landa et al., 2010; Fomel and Kazinnik, 2013; Schwarz et al., 2014b). All of these traveltime approximations have in common that they can be derived from geometry, namely by assuming an analytical reflector shape and a constant velocity overburden. Inspired by the work of de Bazelaire (1988) and Höcht et al. (1999), Schwarz et al. (2014a) found that all non-parabolic operators can in fact be described in two types of auxiliary constant velocity media, which both account for heterogeneity by a unique mechanism. Schwarz et al. (2014a) suggested a simple recipe to transform an effective medium operator, like the classical NMO hyperbola (Mayne, 1962), to its time-shifted counterpart in the optical domain. As a result, the often misleading comparison of the hyperbolic CRS formula and the double-square-root multifocusing expression (Gelchinsky et al., 1999) gets a clear explanation.

In this work, we continue this way of unification by providing the inverse transformation from the optical domain to the effective medium. In this context, we introduce generalized moveout expressions, where the auxiliary medium can be chosen by the user, by supplying the according substitutions. Supported by simple and complex synthetic data examples we find that the double-square-root operators, when being expressed in the same auxiliary medium, can be considered equivalent descriptions. Furthermore, we find that all differences in performance between the considered moveouts can either be attributed to the order of approximation (i. e., double-square-root or single-square-root), which is connected to the handling of reflector curvature, or to the choice of the auxiliary medium, accounting for overburden heterogeneity. In addition, the joint use of both parameterizations turns out to lead to systematic deviations, which can contribute to diffraction and multiple characterization and separation. Finally, we find that the application of an effective medium diffraction operator, in contrast to its optical counterpart, delivers an estimate of the excitation time of a passive seismic source.

AUXILIARY MEDIA

In the general heterogeneous case, seismic rays do not follow straight paths and wavefronts are not circular, but have a more complicated shape. While prestack depth imaging methods seek to describe the full wavefield with a single global model of the subsurface, time imaging methods like stacking do not aim at describing the global, but the local wavefield with operators, which are only valid in a certain small vicinity of the imaging point. Without loss of generality, one can assume that, as long as we confine ourselves to a reasonably small vicinity of the zero-offset recording location x_0, the prestack traveltimes of an emerging

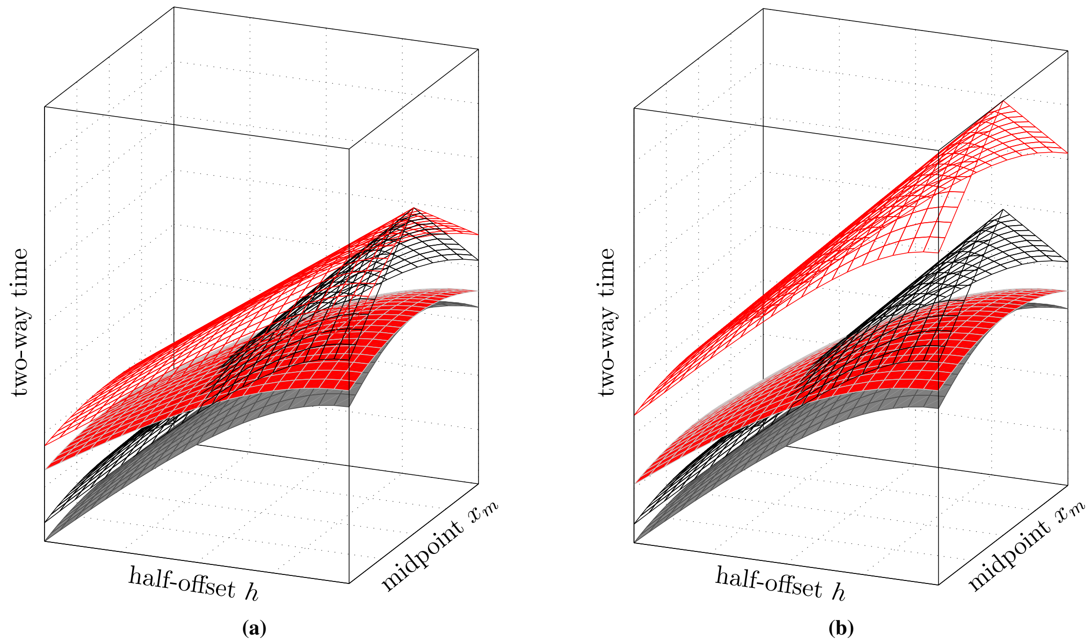

Figure 2: Velocity-shifted CRS moveout (a) and time-shifted CRS moveout (b). Like for the CMP stack, the perturbed moveout surfaces (solid grid) and their asymptotes (hollow grid) are shown in red color.

wavefront can be described by the truncated Taylor series expansion,

$$t(\Delta x_m, h) \approx t_0 + a\Delta x_m + b\Delta x_m^2 + ch^2 \quad , \tag{1}$$

where $\Delta x_m = x_m - x_0$ and h denote midpoint separation and half-offset between source and receiver, respectively. The zero-order term t_0 is the traveltime of the wavefront at the observational coordinate x_0. The first- and second-order coefficients a, b, and c represent slope and curvatures of the traveltime surface $t(\Delta x_m, h)$ recorded in the vicinity of x_0 (see, e.g., Schleicher et al., 1993). According to arguments from paraxial ray theory and by assuming constant velocity v_0 near the recording surface, Hubral (1983) showed that these coefficients can be related to the local properties of two conceptual one-way waves, representing a fictitious exploding point source and an exploding reflector experiment located at the normal incidence point (NIP) on the imaged reflector,

$$a = \left.\frac{\partial t}{\partial x_m}\right|_{(x_m=x_0,h=0)} = \frac{2\sin\alpha}{v_0} \quad , \tag{2}$$

$$b = \frac{1}{2}\left.\frac{\partial^2 t}{\partial x_m^2}\right|_{(x_m=x_0,h=0)} = \frac{\cos^2\alpha}{v_0 R_N} \quad , \tag{3}$$

$$c = \frac{1}{2}\left.\frac{\partial^2 t}{\partial h^2}\right|_{(x_m=x_0,h=0)} = \frac{\cos^2\alpha}{v_0 R_{NIP}} \quad . \tag{4}$$

According to these expressions, in connection with the parabolic formula (1), the traveltime of the reference ray t_0 has no influence on the traveltime differences following from the inclination and curvature of the conceptual waves, i. e. the traveltime moveout, in the frame of this approximation, solely depends on the first- and second-order CRS attributes (Hubral, 1983),

$$t - t_0 = \Delta t(\alpha, R_{NIP}, R_N) \quad . \tag{5}$$

To make maximum use of information redundancy in the data, stacking methods seek to include higher offsets, which, in principle implies a need for additional higher-order terms in the traveltime operator

(1). Since a higher dimensionality of the traveltime fit may lead to instabilities and to undesired additional computational costs, several non-parabolic approximations have been introduced (e.g., Landa et al., 2010; Fomel and Kazinnik, 2013; Schwarz et al., 2014b), which all have in common that the number of degrees of freedom is not increased. In the following subsection we will show that, provided lateral velocity changes are small, these higher-order moveout approximations can account for heterogeneity by two different mechanisms, both relying on the assumption of an auxiliary medium of constant velocity.

Shift in time or in velocity?

Without loss of generality but for the sake of mathematical simplicity, we will first rederive the classical NMO hyperbola, which had a significant impact in the development of stacking methods in seismic processing (Mayne, 1962; Hertweck et al., 2007). For the simple case of one planar horizontal reflector below an overburden of constant velocity v, the exact traveltime moveout expression can be gained from geometry, and, according to the Pythagorean theorem may be expressed as

$$\Delta t = \sqrt{\left(\frac{2R}{v}\right)^2 + \left(\frac{2h}{v}\right)^2} - \frac{2R}{v} \quad , \tag{6}$$

with R denoting the distance from the central midpoint location to the reflector (see Figure 3(a)). As can be inferred from Figure 1(a)) the medium velocity v is responsible for the slope of the hyperbolas asymptote, resembling the direct wave traveltime. While, especially in the context of exploration in sedimentary settings, the assumption of a planar target reflector is often reasonable, the absence of velocity changes in the overburden seems physically not well motivated and generally unrealistic.

In order to be able to stick to the simple mathematical construct (6) and the geometrical appealing picture of straight rays, the allowance for a constant shift in velocity δv seems the most intuitive approach to deal with heterogeneity in the medium. Following from this velocity shift (as indicated in Figure 1(a)), the traveltime moveout is perturbed and the connected asymptote changes its slope. Accordingly, the traveltime moveout is now described in a medium with the effective velocity $v_{shift} = v + \delta v$:

$$\Delta t_v = \Delta t(t_0, v_{shift}) = \sqrt{t_0^2 + \frac{4h^2}{v_{shift}^2}} - t_0 \quad , \tag{7}$$

where t_0 is the zero-offset two-way traveltime, which does not relate to the actual reflector depth R anymore (compare Figure 3(a) and 3(b)). In practice, the approach of shifting the velocity to optimally fit the data is commonly known as velocity analysis (Taner and Koehler, 1969) and has been applied successfully for half a century. In the late eighties, de Bazelaire (1988), motivated by the concept of projections in geometrical optics, introduced an alternate way to maintain the picture of straight rays in a complex medium. In contrast to classical velocity analysis, he proposed that the reference time rather than the velocity should be shifted when heterogeneity occurs in the overburden, i. e.,

$$\Delta t_t = \Delta t(t_{shift}, v_0) = \sqrt{t_{shift}^2 + \frac{4h^2}{v_0^2}} - t_{shift} \quad , \tag{8}$$

with $t_{shift} = t_0 + \delta t$. As Figure 1(b) illustrates, the hyperbola's asymptote changes its overall position in time, but its slope is maintained during this perturbation. Both operations, a constant shift in time and in velocity, results in a similar adaption of the hyperbolic moveout, and for short offsets, these approaches lead to similar results. Nevertheless, we will show in the cause of this work that noticeable systematic deviations between these approximations occur for higher offsets and a higher degree of heterogeneity in the overburden. Following this brief reintroduction of the two different mechanisms to account for heterogeneity for the classical CMP hyperbola, we argue that the preceding findings also apply to the more general CRS stacking concept. In addition, we suggest a simple and, in the context of auxiliary media, more intuitive parameterization, that allows for a generalized definition of higher-order moveouts.

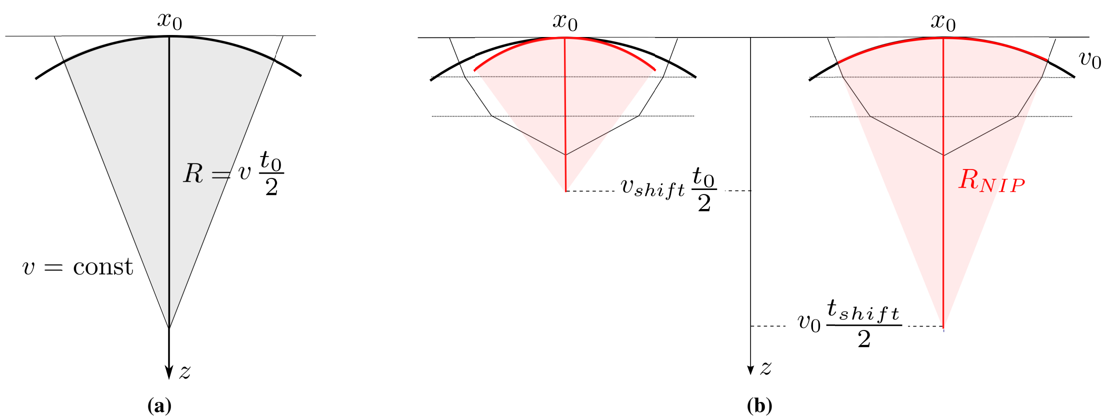

Figure 3: Illustration of the relationship between wavefront curvature and reference traveltime. In case of a single planar target reflector with constant velocity overburden (a), the wavefront curvature R and the distance to the reflector coincide and the hyperbolic approximation is exact, while they differ for the heterogeneous case (b). The solid black lines represent the actual raypath, whereas red color indicates the velocity shift and time shift mechanism, respectively.

CRS stack and complex media

The common-reflection-surface (CRS) stack by Jäger et al. (2001) can be viewed as a generalization of the classical CMP stack to neighbouring CMPs. As a consequence, as can also be inferred from equations (2) to (4), the number of degrees of freedom to fit the moveout surface to the data increases from two to four. Having been introduced in the context of migration (Hubral, 1983), the CRS attributes α, R_{NIP}, and R_N contain both geometrical properties of the imaged reflector and propagation effects due to the overburden. According to the NIP-wave theorem (Hubral et al., 1980; Hubral, 1983), hyperbolic moveout with half-offset h, i. e., in the CMP gather, does not depend on the curvature of the reflector, which is why curvature is not accounted for in formulae (7) and (8). In midpoint direction, however, reflector curvature is a lower, i. e., second-order effect and generally has a strong impact on the traveltime differences of neighbouring rays (see equations (1) and (3)).

In the following, we suggest an alternative to the conventional CRS parameterization by making use of the fact that certain combinations of the CRS parameters remain unaffected by the choice of the auxiliary medium. While in conventional CRS the reflector curvature is related to the parameter R_N, we now suggest to instead use the combination

$$\rho = \frac{R_{NIP}}{R_N} \quad , \tag{9}$$

since it remains unchanged, when we go from the constant near-surface velocity medium of the time shift to the effective constant velocity medium underlying the approach of shifting the velocity and vice versa. In addition, the horizontal slowness or ray parameter

$$p_{0x} = a = \frac{\sin\alpha}{v_0} \quad , \tag{10}$$

according to equation (2) and following from intuition, should be independent of the choice of the auxiliary medium, since it describes the midpoint (i.e. zero-offset) slope of the actual reflection event in the vicinity of measurement location x_0. The shifted zero-offset traveltime represents the reference time of the projected problem and therefore is defined in the auxiliary medium of constant near-surface velocity. As can be concluded from geometry (see Figure 3(b)), it bears a close connection to the NIP wave radius,

$$t_{shift} = \frac{2R_{NIP}}{v_0} \quad , \tag{11}$$

and, as a consequence, following from this geometrical reasoning, links the zero-order and the second-order terms of expansion (1). The relationship of the shifted velocity to the CRS attributes was already established, e.g. by Mann (2002) by identifying it in the reduced hyperbolic CRS formula for diffractions, or independently by Schwarz (2011) by matching the expansion coefficients of the suggested geometrical implicit CRS approach to the coefficients (2) to (4). Following the choice of the horizontal slowness as an independent parameter, this velocity can be defined in slowness notation, which seems more consistent and turns out to simplify expressions

$$p_{shift}^2 = \left(\frac{1}{v_{shift}}\right)^2 = p_{0x}^2 + \frac{t_0}{t_{shift}}\left(p_0^2 - p_{0x}^2\right) \quad , \tag{12}$$

where $p_0 = 1/v_0$. Since in this formula, the shifted velocity is linked to the time shift of the projection approach, and, in accordance with the early work by de Bazelaire (1988), who motivated the use of concepts from geometrical optics, we consider it a *generalized osculating equation*, which is also valid in the CRS framework (compare Figure 2(a) and Figure 2(b)). In the next section, we parameterize the hyperbolic CRS formula (e.g., Jäger et al., 2001), the nonhyperbolic implicit CRS (Schwarz et al., 2014b), and multifocusing (Gelchinsky et al., 1999) by means of the above suggested substitutions (9) to (12).

GENERALIZED MOVEOUTS

For the two different representations of the CMP hyperbola (7) and (8), it becomes immediately obvious that a simple exchange $(t_0, v_{shift}) \leftrightarrow (t_{shift}, v_0)$ transforms the initial operator to the other representation. We conclude from this fact that each moveout expression can be written in a generalized form, i. e., for a general auxiliary medium of constant velocity $\hat{v}$ with its respective reference time $\hat{t}_0$. Depending on the choice of $(\hat{t}_0, \hat{v})$, this generalized moveout $\Delta\hat{t}$ has *two faces*, one accounting for heterogeneity by means of a time shift, the other making use of an effective overburden velocity:

$$(\hat{t}_0, \hat{v}) = \begin{cases} (t_0, v_{shift}) & , \\ (t_{shift}, v_0) & . \end{cases} \tag{13}$$

We would like to emphasize in this context that the choice of either the effective or the near-surface velocity for the auxiliary medium directly implies the corresponding reference traveltime. This connection is expressed by the generalized osculating equation (12), which can be rewritten as

$$\hat{p}^2 = p^2(\hat{t}_0) = p_{0x}^2 + \frac{\hat{t}_0}{t_{shift}}\left(p_0^2 - p_{0x}^2\right) = \begin{cases} p_{shift}^2 & \text{for } \hat{t}_0 = t_0 \quad , \\ p_0^2 & \text{for } \hat{t}_0 = t_{shift} \quad . \end{cases} \tag{14}$$

As will be supported by data examples in the next section, the dependence of moveout on the actual imaging traveltime t_0 has striking implications, like, in particular, the effect of moveout strech after NMO correction or the potential for source time inversion in passive seismic monitoring. In the following, we introduce generalized versions of the CRS, implicit CRS (i-CRS), and multifocusing operators and reveal in which auxiliary medium they were originally formulated.

Hyperbolic moveout

The CRS stack is a natural generalization of the CMP stack, in which redundant information from neighbouring CMP gathers is exploited in the stacking process. Due to this incorporation of adjacent CMPs, the according moveout is a surface rather than a curve, like in the classical CMP stack. Although the parabolic formula (1), being equivalent to the a truncated second-order Taylor series expansion of the traveltime, seems the most natural choice, most implementations appearing in literature are based on a hyperbolic expression (Schleicher et al., 1993; Jäger et al., 2001), in our notation

$$\Delta\hat{t} = \Delta t(\hat{t}_0, \hat{p}) = \sqrt{(\hat{t}_0 + 2p_{0x}\Delta x_m)^2 + 4(\hat{p}^2 - p_{0x}^2)(\rho\Delta x_m^2 + h^2)} - \hat{t}_0 \quad . \tag{15}$$

Similar to the classical CMP stack, numerical investigations as well as application in actual sedimentary environments (e.g., Jäger, 2011) support the notion that the hyperbolic CRS moveout is more suited than the parabolic formula when the subsurface consists of a mostly horizontally layered system. Although it has been introduced via squaring the parabolic expression (1) (e.g., Schleicher et al., 1993), gained from paraxial ray theory (with subsequent neglection of terms of higher order than two), we argue that expression (15) can also be derived from geometry (Schwarz, 2015). For confinement to the CMP gather and vanishing reflector inclination, i.e. $p_{0x} = 0$, the generalized hyperbolic CRS expression reduces to the generalized CMP moveout,

$$\Delta\hat{t} = \Delta t(\hat{t}_0, \hat{p}) = \sqrt{\hat{t}_0^2 + 4\hat{p}^2 h^2} - \hat{t}_0 \quad , \tag{16}$$

which, depending on the choice of reference time $\hat{t}_0$ and, in consequence the auxiliary medium, reduces either to formula (7) or (8). It is interesting to note that, similar to the nonhyperbolic higher-dimensional moveouts discussed in the following subsection, the hyperbolic CRS formula (15) is exact for a certain subsurface model, which in this case constitutes of a planar dipping target reflector beneath a constant velocity overburden (Schleicher et al., 1993). Both formulae, the hyperbolic CRS (15) and the classical CMP hyperbola were first formulated in the effective constant velocity auxiliary medium, which is why their moveout correction depends on the reference time t_0 and therefore also may result in wavelet stretch after correction. While the second face of the CMP hyperbola was already suggested by de Bazelaire in the late eighties (de Bazelaire, 1988), the time-shifted version of hyperbolic CRS was briefly mentioned only in the work of Höcht et al. (1999) and now finds its solid theoretical foundation in the frame of the auxiliary media interpretation of higher-order moveouts.

Nonhyperbolic moveout

Coexisting with the hyperbolic CRS method for fifteen years, the multifocusing approach (Gelchinsky et al., 1999) is based on a double-square-root expression for the reflection traveltime moveout. In contrast to the hyperbolic CRS formula (15), this moveout can be derived from geometry and therefore intrinsically relies on the assumption of straight rays (e.g., Landa et al., 2010). Due to the higher mathematical complexity, the multifocusing moveout has not gained sufficient attention for a long time (e. g. Tygel et al., 1999), but became increasingly important to the community with the rise of interest in imaging diffracted seismic events (Landa et al., 2010). Although it is based on the same kinematic attributes as the CRS method, namely α, R_{NIP}, and R_N, it turns out to noticeably deviate from the hyperbolic approximation when reflectors are curved and when the overburden is heterogeneous (e.g., Schwarz et al., 2014b). In this work, we seek to demystify the role of the multifocusing moveout by reformulating it in a general constant velocity auxiliary medium. By making use of substitutions (9) to (12), we end up with the following generalized form of the multifocusing moveout,

$$\Delta\hat{t} = \Delta t(\hat{t_0}, \hat{p}) = t_s + t_g - \left(\frac{\rho - \sigma^2}{\rho^2 - \sigma^2}\right)\hat{t}_0, \tag{17}$$

where the traveltime contributions t_s and t_g are connected to the downgoing and upgoing segments of the reflected ray,

$$t_s = \sqrt{\left[\left(\frac{1+\sigma}{\rho+\sigma}\right)\frac{\hat{t}_0}{2} + p_{0x}\Delta x_s\right]^2 + (\hat{p}^2 - p_{0x}^2)\Delta x_s^2} \quad , \tag{18}$$

$$t_g = \sqrt{\left[\left(\frac{1-\sigma}{\rho-\sigma}\right)\frac{\hat{t}_0}{2} + p_{0x}\Delta x_g\right]^2 + (\hat{p}^2 - p_{0x}^2)\Delta x_g^2} \quad . \tag{19}$$

The so-called focusing parameter σ is a function of the source and receiver offsets $\Delta x_s = x_s - x_0$ and $\Delta x_g = x_g - x_0$ and therefore changes for each individual ray considered in the vicinity of the central ray observed at midpoint x_0. In the most commonly used planar approximation (Gelchinsky et al., 1999;

Landa et al., 2010), it reads

$$\sigma = \frac{\Delta x_s - \Delta x_g}{\Delta x_s + \Delta x_g + 4\Delta x_s \Delta x_g \, p_{0x} \, \hat{t}_0^{-1}} \quad . \tag{20}$$

Please observe that, in contrast to the hyperbolic CRS approach and its classical CMP hyperbola subset, which almost exclusively appear as effective medium representations in literature (Schwarz et al., 2014a), multifocusing originally describes the projected problem observed in the constant near-surface velocity medium. Therefore, it appears in literature in time-shift parameterization.

Starting from geometrical considerations, similar to the multifocusing approach, Schwarz (2011) and Schwarz et al. (2014a) observed that the nonhyperbolic double-square-root type i-CRS operator can be represented not only in one but two auxiliary domains. While the velocity-shifted effective medium representation turns out to behave similarly to CRS for moderate reflector curvatures and mostly vertical velocity changes in the overburden, the time-shifted version showed a strikingly strong resemblance to multifocusing, theoretically, and backed up by data examples, for the case of high reflector curvatures and in the diffraction limit. Similar to the multifocusing approach, i-CRS treats the down- and up-going contributions of the approximated raypaths separately. In its generalized form it reads

$$\Delta\hat{t} = \Delta t(\hat{t_0}, \hat{p}) = t_s + t_g - \hat{t}_0 \quad . \tag{21}$$

The traveltime contributions t_s and t_g, similar to the multifocusing approach (17) are mathematically complex hyperbolic approximations of the source and receiver traveltimes in the generalized auxiliary medium of constant slowness $\hat{p}$,

$$t_s = \sqrt{\left[\frac{1}{\rho}\frac{\hat{t}_0}{2} + p_{0x}\Delta x_s\right]^2 + \left(\hat{p}^2 - p_{0x}^2\right)\Delta x_s^2 - \left(\frac{1}{\rho} - 1\right)\hat{t}_0\,\hat{p}\,\sin\theta\Delta x_s + d} \quad , \tag{22}$$

$$t_g = \sqrt{\left[\frac{1}{\rho}\frac{\hat{t}_0}{2} + p_{0x}\Delta x_g\right]^2 + \left(\hat{p}^2 - p_{0x}^2\right)\Delta x_g^2 - \left(\frac{1}{\rho} - 1\right)\hat{t}_0\,\hat{p}\,\sin\theta\Delta x_g + d} \quad , \tag{23}$$

where d is a correction term for the finite reflector curvatures,

$$d = \left(\frac{1}{\rho} - 1\right)\left(\frac{\hat{t}_0}{2}\right)^2 \left[\frac{1}{\rho}\left(1 - \frac{2}{\hat{p}}\left(p_{0x}\sin\theta + \sqrt{\hat{p}^2 - p_{0x}^2}\cos\theta\right)\right) - 1\right] \quad . \tag{24}$$

Please note that this contribution vanishes for the diffraction case, where $\rho = R_{NIP}/R_N = 1$. Solving the Problem of reflection from a circular reflector in a constant velocity medium, i-CRS iterates for the angle θ, which geometrically represents the angle defining the finite-offset reflection point. It therefore plays a similar role as the focusing parameter (20) in connecting traveltime contributions of the up- and down-going ray segments,

$$\tan\theta = \frac{p_{0x} + \rho\,\hat{p}^2\,\hat{t}_0^{-1}}{\sqrt{\hat{p}^2 - p_{0x}^2}} \left(\Delta x_s + \Delta x_g + (\Delta x_s - \Delta x_g)\frac{t_s - t_g}{t_s + t_g}\right) \quad . \tag{25}$$

At this point, we would like to emphasize the special role of the multifocusing moveout, which, in contrast to all other presented methods, like CRS and i-CRS, was originally formulated in the constant near-surface velocity medium and therefore, like the shifted hyperbola by de Bazelaire (1988), relies on a time-shift to account for heterogeneity. Without commenting on the auxiliary medium itself, Landa (2007) already stated that the multifocusing moveout correction does not suffer from moveout stretch (since it does not depend on the reference traveltime t_0) and reduces to the time-shifted hyperbola by de Bazelaire in the CMP gather, when the overburden consists of a horizontally layered system. With this work, we seek to properly define the unique role of the multifocusing approach and argue that it behaves completely equivalent to other double-sqare-root expressions, like the considered i-CRS operator, when viewed in the same auxiliary medium.

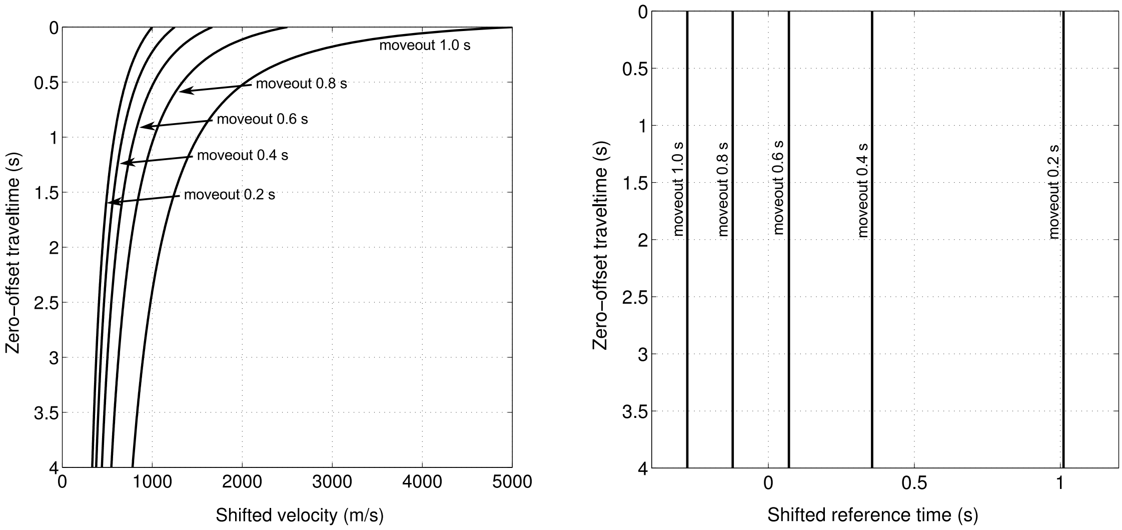

(a) (b)

Figure 4: Iso-moveout curves for the velocity-shifted classical NMO hyperbola (a) and the time-shifted hyperbola by de Bazelaire (b) for a fixed finite-offset. Although of higher dimensionality, similar dependencies also apply for the surface-based CRS, i-CRS, and multifocusing stack.

Since both, generalized multifocusing and generalized i-CRS, reduce to exactly the same expressions for planar horizontal layering in the CMP gather or the increasingly important diffraction case, we consider them being of comparable accuracy. Both operators reduce to the exact solution for one single planar reflector (in the CMP gather) and for a point diffractor with a constant velocity background. This supports the finding that all higher-order expressions with the same number of degrees of freedom as the parabolic formula (1), i.e. hyperbolic CRS, i-CRS or multifocusing, are exact for a certain subsurface model and can also be derived from geometry. Please note that these approaches, in consequence, are confined by an asymptotic curve or surface (illustrated in figures 1(a) to 2(b)). The parabolic formula neither has two faces, like the higher-order expressions, nor does an asymptote exist and it happens to be never exact, no matter how simple the model is chosen (Schwarz, 2015).

Since all presented generalized moveouts, for small vicinities, i.e. up to second order, are equivalent to the parabolic formula (1), and due to the fact that the two double-square-root expressions are capable of handling low and high reflector curvatures equally well provided that lateral velocity changes are moderate, we consider either generalized i-CRS or multifocusing as the most general moveout expression in this context. As we will show in the following section, these theoretical notions can also be clearly supported in actual data application. In addition, we will show that the existence of two faces for the higher-order moveouts, besides unification, also bears strong potential for wavefield characterization.

IMPLICATIONS AND APPLICATIONS

Moveout stretch

As already indicated in the theory section, the choice of the auxiliary medium directly implies the choice of a specific conceptually different mechanism to account for heterogeneity. Due to the fact that the effective medium moveouts all have in common that they directly depend on the zero-offset reference traveltime t_0, moveout stretch can be observed for all these approaches. It is interesting to note that this effect, however, may also show for data modeled in a hypothetical medium of perfectly constant velocity (see, e. g., Perroud and Tygel, 2004). For the sake of simplicity, we demonstrate this behavior for the hyperbolic CMP moveout (16) only, but we would like to stress that the presented findings also apply to the more general multi-dimensional CRS-type methods. Figures 4(a) and 4(b) show *iso-moveout* curves, i.e. curves of constant moveout, for the velocity-shifted CMP hyperbola and its time-shifted counterpart for a fixed finite-offset.

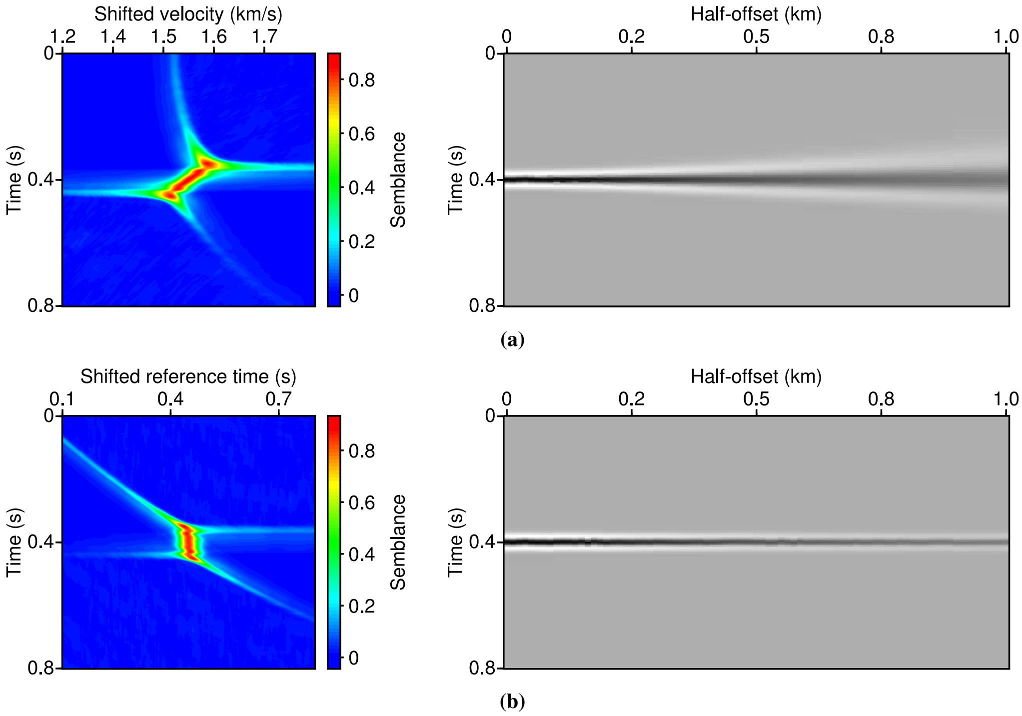

Figure 5: Illustration of the moveout stretch (a), resulting from the dependency of the velocity-shifted moveout on the reference time along the wavelet. The time-shifted moveout correction (b), even for higher offsets, does not result in stretching of the signal.

Presented are five different constant moveouts with the shifts in velocity and in time as functions of the reference traveltime t_0. By comparing 4(a) and 4(b) we observe that in order to describe one particular moveout for different reference traveltimes t_0, the shift in velocity needs to be changed, whereas time shift moveouts remain constant for the whole range of reference traveltimes, and, therefore do not depend on t_0. This implies that in order to describe the moveout as a constant along the recorded seismic wavelet, the velocity shift needs to be changed according to the operator's iso-moveout curve.

In consequence, the intuitive choice of a constant velocity-shift for one event results in neglection of the slope of the velocity-shift iso-moveout curve along the wavelet leads to overcorrections for some parts and undercorrections for others, resulting in an undesired increase of the signal period at higher offsets. As may be concluded from Figure 4(a), this effect is generally most pronounced at shallow times t_0, whereas it becomes almost negligible for higher values of t_0. As can also be inferred from Figure 4(b), the time-shifted moveouts do not show this dependency and the intuitive choice of a constant time-shift for a single event leaves the frequency content unchanged. Figure 5(a) and Figure 5(b) demonstrate this with a simple data example, where the measured event of a single shallow planar horizontal layer is corrected either via the correct medium velocity as shifted velocity (Figure 5(a)) or the corresponding correct reference traveltime as the shifted traveltime. One can clearly observe the effect of moveout stretch for the velocity shift approach, whereas this phenomenon does not show for the time shift mechanism.

Heterogeneity and diffractions

Schwarz (2011) and Schwarz et al. (2014a) concluded from simple and even moderately complex synthetic data examples that the choice of the auxiliary medium for the i-CRS operator resulted in sometimes pronounced differences in achieved quality of fit and the connected CRS attribute estimation. In this subsection, we seek to systematically investigate the performance of the time shift and the velocity shift mechanism to account for overburden heterogeneity. To ensure realistic circumstances and sufficient applicability of the resulting conclusions, we choose the complex BP 2004 Velocity Benchmark (Billette

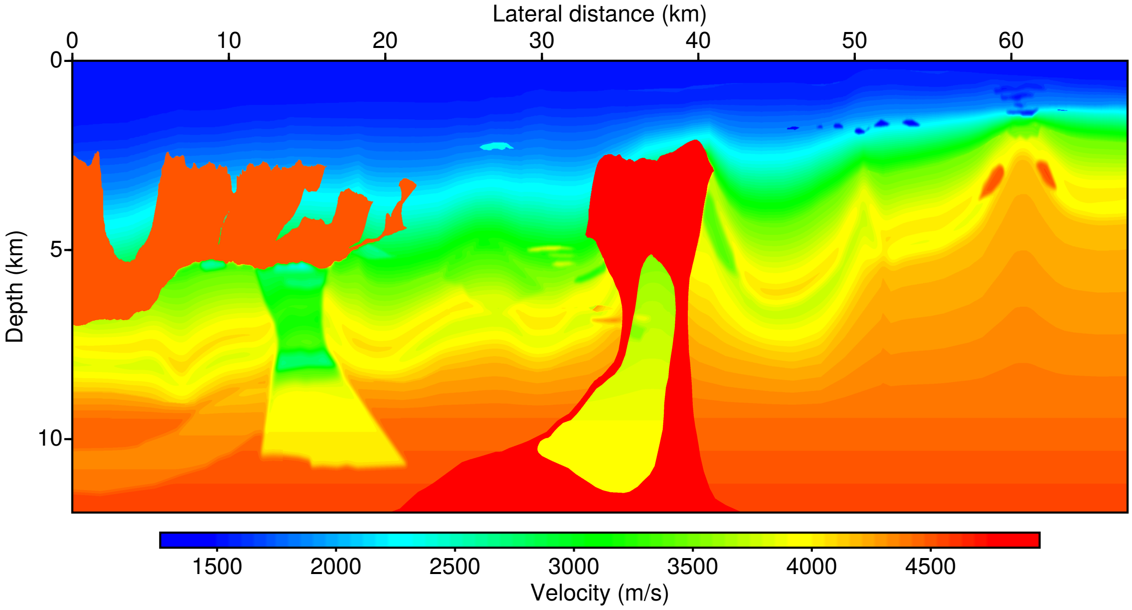

Figure 6: The 2004 BP Velocity Benchmark model. While the left side of the model is dominated by complicated diffracting structures, the right side exhibits strong velocity gradients.

and Brandsberg-Dahl, 2005), since it contains all relevant geological features that can lead to higher-order effects in the traveltime moveout. Figure 6 shows the BP model with its wide range of velocity gradients and complex features like a salt-body system on the left and shallow strong vertical velocity changes on its right. Resulting from the model, as can be observed in the top of Figure 7, the velocity-shifted i-CRS-stacked ZO section of the BP multi-coverage data shows very pronounced and complex diffraction patterns in the left part and strong surface-related multiple reflections in the right part.

To clearly emphasize the differences of the two faces of the suggested generalized operators, and to motivate some potential applications of their simultaneous use, we here confine ourselves to the comparison of the CRS attributes α, and R_{NIP}, which turn out to either efficiently characterize diffractions or velocity changes in the model. The bottom of Figure 7 shows the angle estimate difference of the two versions of the i-CRS operator on the left and the corresponding deviations in R_{NIP} on the right. As can be inferred from these deviation patterns, the angle differences are only non-negligible for events stemming from highly curved structures like the complex rugged top-of-salt being present in the left side of the model, whereas differences in R_{NIP} seem to indicate the general presence and the strength of velocity variations in the overburden. Please note that the surface-related multiple reflections are not affected by velocity changes in the subsurface and can therefore be clearly distinguished from the primary reflections whose rays were exposed to the heterogeneity of the shallow layers in the model. Although not stressed here, simple quantitative studies on synthetic data indicated that velocity-shifted operators tend to estimate the CRS attributes more accurately than their time-shifted counterparts when the heterogeneity of the overburden increases (Schwarz, 2011).

Figure 8 and Figure 9 show two closeups of Figure 7 (indicated by frames) for all three multi-parameter operators considered in this paper. One can clearly observe the strong systematics in the attribute deviations, which, for the case of the nonhyperbolic double-square-root operators i-CRS and multifocusing, only show, when a time-shifted version is compared with an expression shifted in velocity. The time-shifted face of the i-CRS operator turns out to estimate the attributes absolutely equivalently to the multifocusing formulation, which only appears in time-shifted notation in existing literature (e.g., Gelchinsky et al., 1999). In accordance, the estimate differences vanish, when we compare the effective medium version of i-CRS, which was suggested by Schwarz et al. (2014b), with the new effective medium (velocity-shifted) formulation of multifocusing. The same systematics also show for the hyperbolic CRS operator, indicating that the generalized operators have the potential to provide additional insight into the character and physical origin

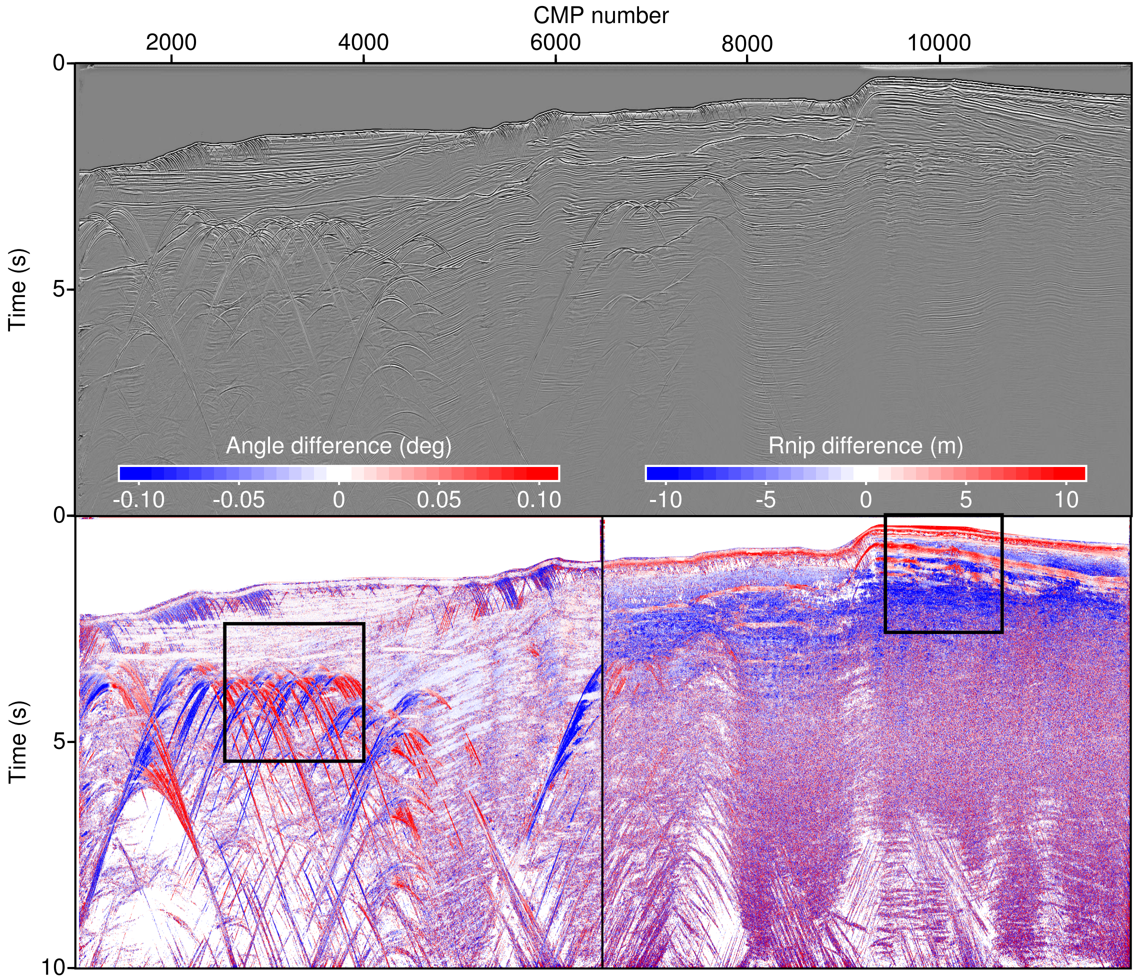

Figure 7: The velocity-shifted i-CRS stack of the 2004 BP Velocity Benchmark data (top) and the respective differences of estimated attributes $\Delta\alpha = \alpha(p_{shift}) - \alpha(t_{shift})$ shown on the left and $\Delta R_{NIP} = R_{NIP}(p_{shift}) - R_{NIP}(t_{shift})$ shown in the right part of the section (bottom). The black frames indicate closeups shown in Figures 8 and 9.

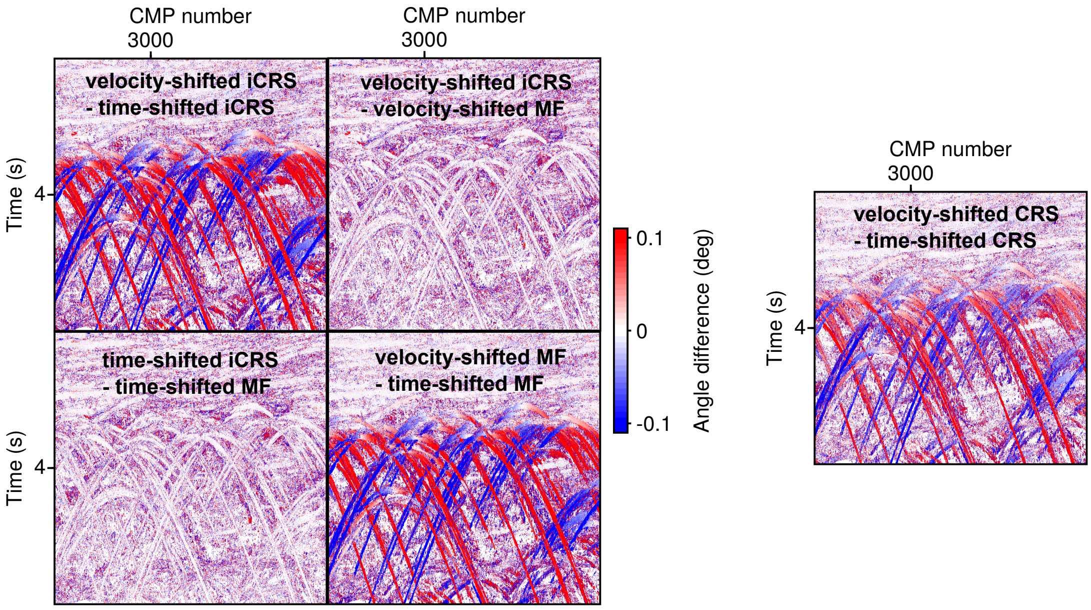

Figure 8: Closeup of the difference section of the emergence angle (α) estimates for CRS, i-CRS, and multifocusing.

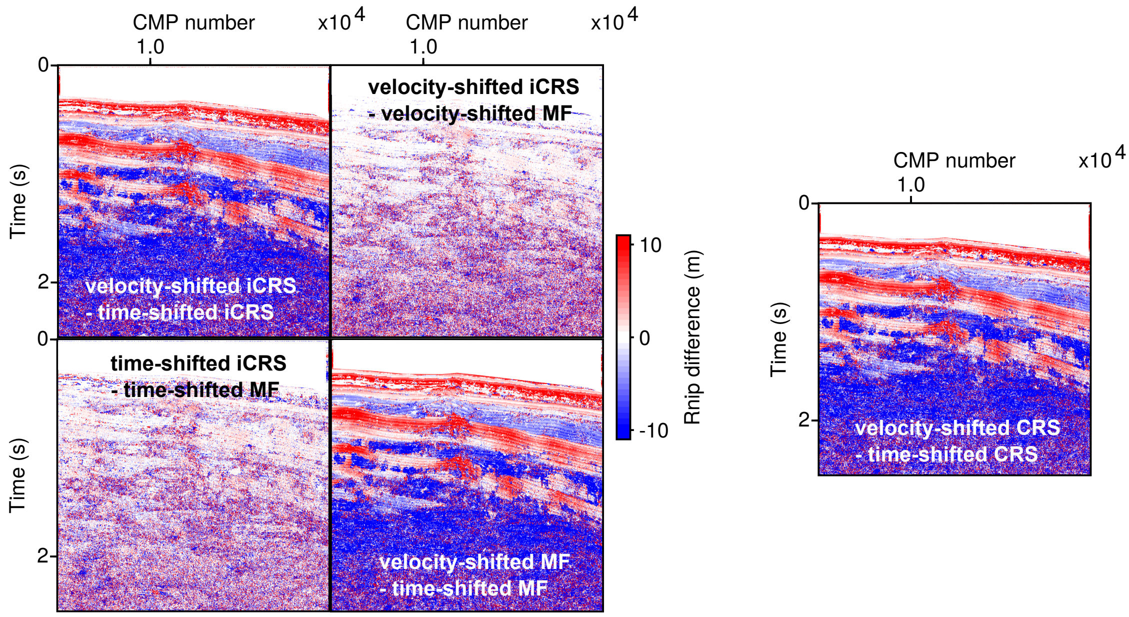

Figure 9: Closeup of the difference section of the NIP wave radius (R_{NIP}) estimates for CRS, i-CRS, and multifocusing.

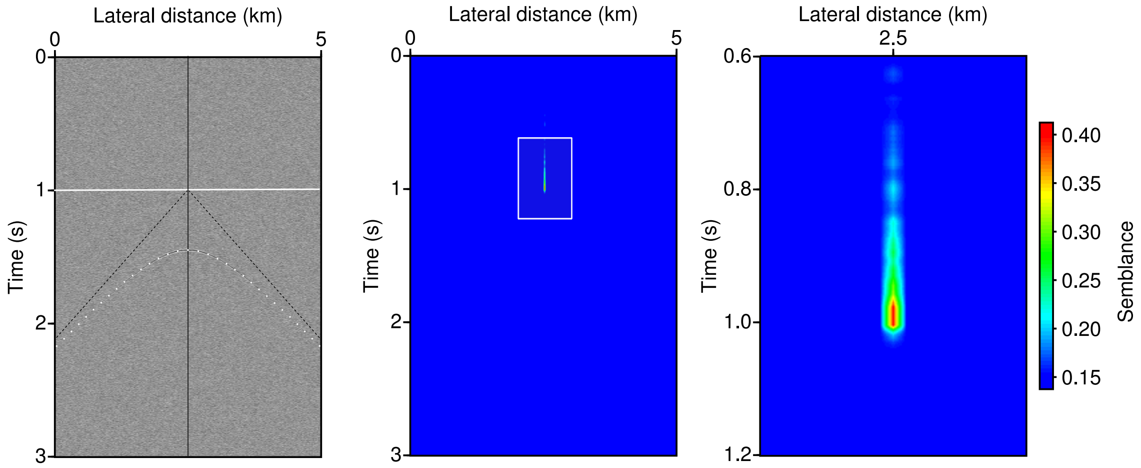

Figure 10: Simple synthetic test of the localization of a diffraction event in time (middle and right). The left panel shows the recorded data with modeling start time and moveout indicated in white and the asymptote, utilised for time localization, denoted by the black dotted line.

of a recorded event.

Passive seismics

In the context of moveout traveltime correction we found that the undesired effect of moveout stretch is an inherent property of the velocity-shifted representation of each operator, whereas wavelets remain undistorted for the time-shift mechanism. In this final part of the paper, we seek to support the notion that both versions of each operator may not only be jointly utilized, but that the velocity-shift mechanism's characteristic dependence on the reference time t_0 may also prove to be advantageous for certain applications. In the context of passive seismic monitoring or earthquake seismology, the localization of the unknown source of a seismic event is a fundamental problem and may be approached with the data-driven method of diffraction stacking (Zhebel et al., 2011). Without loss of generality and supported by a simple synthetic test example, we discuss the possibility of inverting for the passive seismic source time.

The generalized 2D one-way diffraction traveltime in apex notation can be written as

$$t = t_{source} + t_0 + \Delta\hat{t}(\hat{t}_0, \hat{p}) = t_{source} + t_0 + \sqrt{\hat{t}_0^2 + \hat{p}^2 \Delta(x - x_{source})^2} - \hat{t}_0 \quad , \tag{26}$$

where (t_{source}, x_{source}) is the location in horizontal coordinate and time, and x is the horizontal trace location. Please note that for localization of the horizontal position, description of moveout is sufficient and the reference time, according to the time shift mechanism, may be chosen arbitrarily. To also allow for a localization in time, i.e. to estimate the source time, however, only the effective medium approach is suited, since the effective medium moveout directly depends on the true reference time t_0,

$$t = t_{source} + \sqrt{t_0^2 + p_{shift}^2 (x - x_{source})^2} \quad . \tag{27}$$

This means that in order to allow for a localization in time, both, the reference time t_0 and the shifted slowness p_{shift} need to be estimated in a fitting procedure and the stacking result is written to (t_{source}, x_{source}). Figure 10 illustrates the inversion of the source time by treating the reference time t_0 alongside p_{shift} as a free fitting parameter. Shown is a simple synthetic test in which a one-way shot recording is modeled in a constant vertical velocity gradient background $v = v_0 + 0.5\ \mathrm{s}^{-1} z$. To simulate a passive seismic source experiment we artificially added 1 s of extra recording time to the physically modeled data, which we aim to invert for. To simulate a more realistic setting, we also applied Gaussian noise with a signal-to-noise ratio of 0.5 to the data, which is shown in the left panel of Figure 10. As can be observed in the middle and right panel of this figure, the suggested two-parameter diffraction stack for this simple example turns out to allow for a robust inversion of both, the correct horizontal location, and the simulated excitation time of the passive seismic source.

CONCLUSIONS

In this work we showed, that all traveltime operators, which provide the correct solution to a certain subsurface model, may be represented geometrically in an auxiliary medium of constant velocity. While most commonly, effects of heterogeneity are intuitively accounted for by shifting the constant velocity of the auxiliary medium, a shift in the reference time can lead to a similar adaption of the traveltime moveout in the vicinity of a reference ray. Following from these findings and continuing the work of de Bazelaire in the late eighties, we suggest generalized expressions of the classical CMP hyperbola, conventional CRS, and the double-square-root implicit CRS and multifocusing operators, which may be shifted either in velocity or in time. As a consequence, we observed that the two different versions of each operator show systematically different behaviour in the presence of heterogeneity. This generalization revealed that the multifocusing moveout, in contrast to hyperbolic CRS and i-CRS, was originally formulated for the surface projection, where a time-shift accounts for heterogenity. Comparison of double-square-root-based implicit CRS and multifocusing revealed that both operators are essentially equivalent, when the same auxiliary medium for both operators is considered. Application of both versions of an operator for the complex BP 2004 velocity benchmark dataset not only confirmed unification, but also revealed potential for diffraction or multiple identification. While time-shifted moveout corrections generally do not suffer from wavelet stretch, effective operators allow to invert for the true reference traveltime, which can be utilized in passive seismic monitoring. So, in addition to the joint use, each representation turned out to have distinct advantages over the other in particular contexts of application.

ACKNOWLEDGEMENTS

We thank the Applied Seismics Group Hamburg for continuous discussions. This work was partly supported by the sponsors of the Wave Inversion Technology (WIT) Consortium and the project 'Imaging steep structures with diffractions', which is funded by the German Ministry of Environment (BMU 0325363C).

REFERENCES

Billette, F. and Brandsberg-Dahl, S. (2005). The 2004 BP Velocity Benchmark. In *67th EAGE Conference & Exhibition*.

de Bazelaire, E. (1988). Normal moveout revisited – inhomogeneous media and curved interfaces. *Geophysics*, 53:143–157, doi:10.1190/1.1442449.

Fomel, S. and Grechka, V. (2001). Nonhyperbolic reflection moveout of P waves. An overview and comparison of reasons. *CWP-372: Colorado School of Mines*.

Fomel, S. and Kazinnik, R. (2013). Non-hyperbolic common reflection surface. *Geophysical Prospecting*, 61(1):21–27, doi:10.1111/j.1365–2478.2012.01055.x.

Gelchinsky, B., Berkovitch, A., and Keydar, S. (1999). Multifocusing homeomorphic imaging – part 1. Basic concepts and formulae. *Journal of Applied Geophysics*, 42:229–242, doi:10.1016/S0926–9851(99)00038–5.

Hertweck, T., Schleicher, J., and Mann, J. (2007). Data stacking beyond CMP. *The Leading Edge*, 26(7):818–827, doi:10.1190/1.2756859.

Höcht, G., de Bazelaire, E., Majer, P., and Hubral, P. (1999). Seismics and optics: hyperbolae and curvatures. *Journal of Applied Geophysics*, 42:261–281, doi:10.1016/S0926–9851(99)00040–3.

Hubral, P. (1983). Computing true amplitude reflections in a laterally inhomogeneous earth. *Geophysics*, 48:1051–1062, doi:10.1190/1.1441528.

Hubral, P., Krey, T., Larner, K. L., et al. (1980). *Interval velocities from seismic reflection time measurements*. Society of Exploration Geophysicists.

Jäger, R. (2011). *The Common-Reflection-Surface Stack – Theory and Application*. Diploma thesis, University of Karlsruhe.

Jäger, R., Mann, J., Höcht, G., and Hubral, P. (2001). Common-reflection-surface stack: Image and attributes. *Geophysics*, 66:97–109, doi:10.1190/1.1444927.

Khaidukov, V., Landa, E., and Moser, T. J. (2004). Diffraction imaging by focusing-defocusing: An outlook on seismic superresolution. *Geophysics*, 69(6):1478–1490, doi:10.1190/1.1836821.

Landa, E. (2007). *Beyond conventional seismic imaging*. European Association of Geoscientists and Engineers.

Landa, E., Keydar, S., and Moser, T. J. (2010). Multifocusing revisited – inhomogeneous media and curved interfaces. *Geophysical Prospecting*, 58:925–938, doi:10.1111/j.1365–2478.2010.00865.x.

Mann, J. (2002). *Extensions and Applications of the Common-Reflection-Surface Stack Method*. PhD thesis, University of Karlsruhe.

Mayne, W. H. (1962). Common reflection point horizontal data stacking techniques. *Geophysics*, 27:927–938, doi:10.1190/1.1439118.

Perroud, H. and Tygel, M. (2004). Nonstretch NMO. *Geophysics*, 69(2):599–607, doi:10.1190/1.1707080.

Schleicher, J., Tygel, M., and Hubral, P. (1993). Parabolic and hyperbolic paraxial two-point traveltimes in 3D media. *Geophysical Prospecting*, 41(4):495–513, doi:10.1111/j.1365–2478.1993.tb00581.x.

Schwarz, B. (2011). *A new nonhyperbolic multi-parameter stacking operator*. Diploma thesis, University of Hamburg.

Schwarz, B. (2015). *Moveout and Geometry*. PhD thesis, University of Hamburg.

Schwarz, B., Vanelle, C., and Gajewski, D. (2014a). Auxiliary Media-A Generalized View on Stacking. In *76th EAGE Conference and Exhibition 2014*, pages doi:10.3997/2214–4609.20140988.

Schwarz, B., Vanelle, C., Gajewski, D., and Kashtan, B. (2014b). Curvatures and inhomogeneities: An improved common-reflection-surface approach. *Geophysics*, 79(5):S231–S240, doi:10.1190/geo2013–0196.1.

Taner, M. T. and Koehler, F. (1969). Velocity spectra-digital computer derivation applications of velocity functions. *Geophysics*, 34(6):859–881, doi:10.1190/1.1440058.

Tygel, M., Santos, L. T., and Schleicher, J. (1999). Multifocus moveout revisited: derivations and alternative expressions. *Journal of applied geophysics*, 42(3):319–331, doi:10.1016/S0926–9851(99)00043–9.

Zhebel, O., Gajewski, D., and Vanelle, C. (2011). Localization of seismic events in 3D media by diffraction stacking. In *73rd EAGE Conference & Exhibition*, pages doi:10.3997/2214–4609.20149021.